

Electronic and Optical Properties of ZnIn_2Te_4

Biplab Ganguli, Kamal Krishna Saha

Tanusri Saha-Dasgupta and Abhijit Mookerjee

S. N. Bose National Centre for Basic Sciences. Block-JD, Sector-III, Kolkata-700098, India.

A.K.Bhattacharya

Centre for Catalysis and Materials Design, Department of Engineering, University of Warwick, Coventry, U.K.

Abstract. Band structure and optical properties of defect- Chalcopyrite type semiconductor ZnIn_2Te_4 have been studied by TB-LMTO first principle technique. The optical absorption calculation suggest that ZnIn_2Te_4 is a direct-gap semiconductor having a band gap of 1.40 eV., which confirms the experimentally measured value. The calculated complex dielectric-function $\epsilon(E) = \epsilon_1(E) + i\epsilon_2(E)$ reveal distinct structures at energies of the critical points in the Brillouin zone.

E-mail: biplabg@bose.res.in

PACS numbers: 71.20,71,20c

1. Introduction

The ternary semiconducting compounds $A^{II}B_2^{III}C_4^{VI}$ have been widely investigated because of their potential applications in electro-optic, optoelectronic, and non-linear optical devices [1]. Most of these compounds have the defect chalcopyrite or stanite structure [2, 3]. In an $A^{II}B_2^{III}C_4^{VI}$ defect chalcopyrite compound, A, B, and C atoms and the vacancy E, are distributed as follows [3].: A site at $(a/2, 0, c/4)$, B at $(0, 0, c/2)$ and $(0, a/2, c/4)$, C at $(\alpha, \bar{\beta}, \gamma)$, $(\bar{\alpha}, \beta, \gamma)$, $(\beta, \alpha, \bar{\gamma})$ and $(\bar{\beta}, \bar{\alpha}, \bar{\gamma})$ and E at $(0, 0, 0)$. It's lattice parameters are given by $\alpha = \beta = a/4$, $\gamma = c/8$ and $c = 2a$, as shown in the figure 1.

In this communication we shall investigate the electronic structure and optical properties of the defect chalcopyrite $ZnIn_2Te_4$ from a first principles approach. The chosen system is not only important for its application in technology, but is also important for the study of the effect of defect or impurity on various properties of materials. There is also growing interest in the study of defect and nano structures [12, 13]. One of the experimental method for the preparation of nano-structures is to fill in the structural voids in a “host” compound with atoms of a given substance. These structures could either be local void clusters or even tubulary voids. The characteristics dimensions. The host compound helps to form a matrix in which these nano structures stabilize. In a subsequent communication, we shall extend the present work to include nano structures in host materials.

Recently Ozaki *et al* [4, 5] have carried out a detailed experimental and theoretical study of optical properties of amorphous and crystalline $ZnIn_2Te_4$. There are few other experimental measurement [6]- [10] on the compound also but there has been no first principles calculation for the electronic structure and optical properties of this material.

The band structure calculations by empirical parameterized tight-binding methods has been carried out for $ZnIn_2Te_4$ by Meloni *et al* [11] and Ozaki *et al* [5]. These calculations required fitted parameters. The actual crystal structures also seem to have been simplified. Meloni *et al* have assumed a pseudocubic structure (space group = V_d), rather than the actual chalcopyrite type structure. Ozaki *et al* have taken a defect chalcopyrite structure. However, the space group S_4^2 , which they assumed, does not reflect the correct symmetry of this structure. This is the usual chalcopyrite structure but with vacancies at the sites as shown in the figure 1. Because of the vacancies, this structure does not have the full space group S_4^2 . Rather, we can assign this structure the $I\bar{4}$ symmetry. The positions of Te's are zinc-blende type, *i.e.* two inter-penetrating fcc lattices shifted one-fourth of the way along a body diagonal. The values of the lattice parameters a and c are taken from experiment to be 6.11\AA and 12.22\AA respectively as reported by Hahn and Ozaki [2, 5]. The positions of the atoms within the unit cell is shown in table 1.

Atom type	Positions			Atom type	Positions		
Zn	0.00	0.50	-0.50	In1	0.00	0.00	0.00
In2	0.50	0.00	-0.50	Te	0.25	0.25	0.25
Te	0.25	-0.25	-0.25	Te	-0.25	0.25	-0.25
Te	0.25	0.25	-0.75	E1	0.00	0.00	1.00
E2	0.25	0.25	-0.25	E2	0.25	-0.25	0.25
E2	-0.25	0.25	0.25	E2	0.25	0.25	-1.25
E3	0.50	0.00	0.00	E3	0.00	0.50	0.00
E4	0.00	0.00	0.50	E4	0.00	0.00	-0.50

Table 1. Positions within the unit cell of atomic basis, including the empty spheres to take into account the voids within the structure

2. Results and Discussion

2.1. Electronic Structure Calculations

To start with, for our electronic structure calculations we have used the well established tight-binding linearized muffin-tin orbitals method (TB-LMTO), discussed in detail

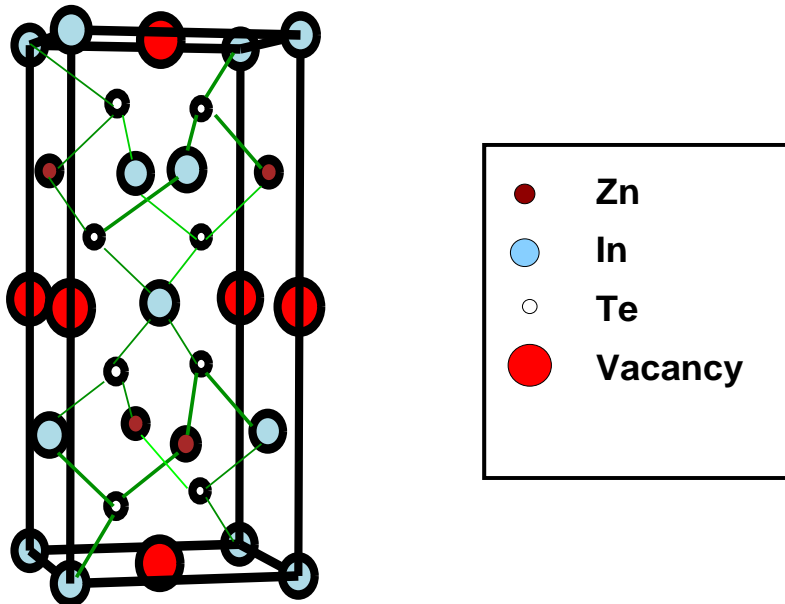


Figure 1. Crystal structure of defect-chalcopyrite-type semiconductor $ZnIn_2Te_4$. Here an orthorhombic primitive cell is shown

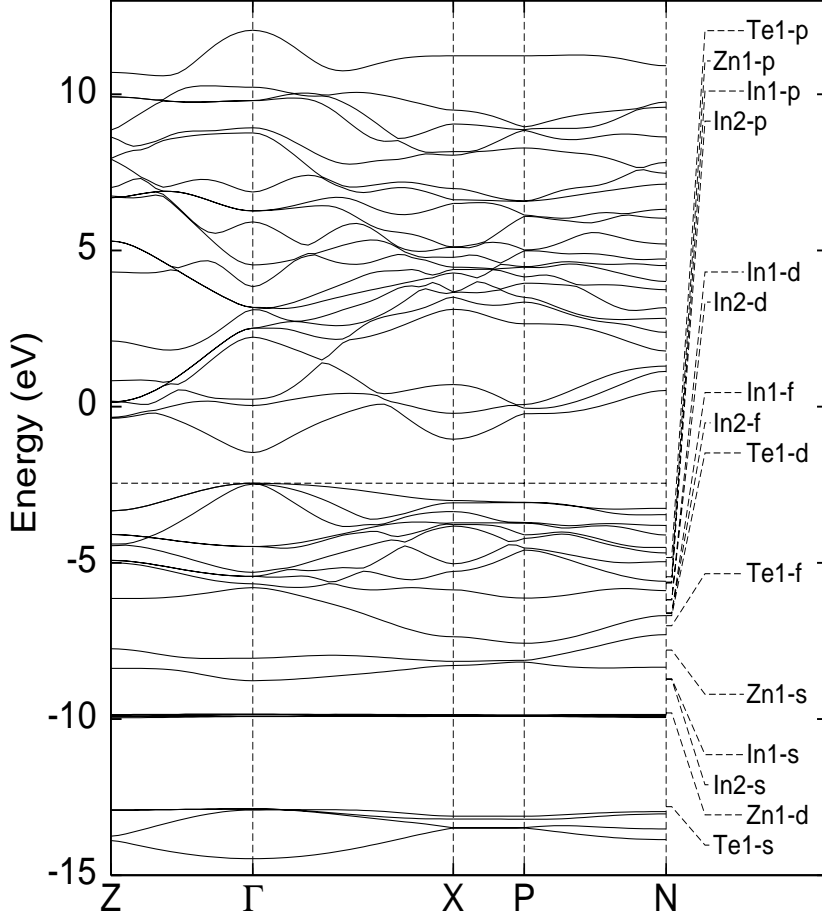


Figure 2. The band structure of $ZnIn_2Te_4$ within the TB-LMTO

elsewhere [16, 17, 19]. Electron correlations are taken within local density approximation of density functional theory [14, 15].

The TB-LMTO energy bands in several high symmetry directions in reciprocal space is shown in figure 2. Let us examine this in some detail. The basis of the TB-LMTO starts from the minimal set of muffin-tin orbitals of a KKR formalism and then linearizes it by expanding around a ‘nodal’ energy point $E_{\nu\ell}^{\alpha}$. The wave-function is then expanded in this basis :

$$\Phi_{j\mathbf{k}}(\mathbf{r}) = \sum_L \sum_{\alpha} c_{L\alpha}^{j\mathbf{k}} \left[\phi_{\nu L}^{\alpha}(\mathbf{r}) + \sum_{L'} \sum_{\alpha'} h_{LL'}^{\alpha\alpha'}(\mathbf{k}) \dot{\phi}_{\nu L'}^{\alpha'}(\mathbf{r}) \right] \quad (1)$$

and,

$$\begin{aligned} \phi_{\nu L}^{\alpha}(\mathbf{r}) &= i^{\ell} Y_L(\hat{r}) \phi_{\ell}^{\alpha}(r, E_{\nu\ell}^{\alpha}) \\ \dot{\phi}_{\nu L}^{\alpha}(\mathbf{r}) &= i^{\ell} Y_L(\hat{r}) \frac{\partial \phi_{\ell}^{\alpha}(r, E_{\nu\ell}^{\alpha})}{\partial E} \end{aligned}$$

$$h_{LL'}^{\alpha\alpha'}(\mathbf{k}) = (C_L^\alpha - E_{\nu\ell}^\alpha) \delta_{LL'} \delta_{\alpha\alpha'} + \sqrt{\Delta_L^\alpha} S_{LL'}^{\alpha\alpha'}(\mathbf{k}) \sqrt{\Delta_{L'}^{\alpha'}}$$

C_L^α and Δ_L^α are TB-LMTO potential parameters and $S_{LL'}^{\alpha\alpha'}(\mathbf{k})$ is the structure matrix.

First note that for the calculation of the optical properties of the solid we need to span a large energy range, from the occupied valence to the unoccupied conduction states. For $ZnInTe$ this spans a range from -15 eV to 10 eV. The “nodal” energies cluster below -5 eV in the valence band. Obviously, the conduction part of the band is not accurately reproduced. The third generation NMTO expands the wavefunction in term of a basis which is expanded as a Lagrange interpolation around a discrete set of *nodal* energies $\{\epsilon_n\}$:

$$\Phi_{j\mathbf{k}}(\mathbf{r}) = \sum_L \sum_\alpha c_{L\alpha}^{j\mathbf{k}} \left[\sum_{n=0}^N \phi_{nL}^\alpha(\mathbf{r}) \mathcal{L}_{n,LL'}^{(N)}(\mathbf{k}) \right] \quad (2)$$

The $\mathcal{L}_{nRL,R'L'}^{(N)}$ are Lagrange matrices which are such that the energy dependent partial wave basis $\phi_L^\alpha(\mathbf{r}, E)$ takes the values $\phi_{nL}^\alpha(\mathbf{r})$ at the *nodal* energies. Unlike the LMTO, the *nodal* energies are independent of the indeces $L\alpha$. By choosing the *nodal* energies across the energy range of interest we can accurately reproduce the bands in that range. This was shown for GaAs in the range -15 eV to 20 eV by Andersen and Saha-Dasgupta [18].

The figure 3 shows the energy bands obtained from the NMTO using three *nodal* energies spread across the energy range of interest. In comparison with the figure 2, we note that the largest change occurs in the conduction band, away from the TB-LMTO nodal energies bunched below -5 eV. We have used the von Barth-Hedin exchange [20] with 512 \mathbf{k} -points in the irreducible part of the Brillouin zone.

The calculated density of states within TB-LMTO and NMTO are shown in the figure 4. It is evident from these two figures that there is significant difference between these two only in the conduction band. From the band structure comparison, this was also evident for the reasons discussed earlier. These densities agree quite well with the experimental XPS measurements of Ozaki *et al* [5] and also with their parametrized tight-binding calculations. These results are shown in the figure 5. It must be noted here that since these calculations are based on the LDA, we do obtain a lower band gap. In this case the NMTO estimate of the band gap is around 1.3 eV, while the XPS data indicate a gap of around 2 eV. Nor can we have much confidence about the conduction bands. This problem can be tackled more accurately, for example, through by quasi-particle band structure within a GW type approximation [27]. These NMTO based calculations are a much better starting point of GW self-consistency iterations than the first or second generation LMTOs (see comments in [18])

The TB-LMTO band structure gives us insight into the various structures in the density of states. At the lowest energies around -14 eV we have the states arising out of

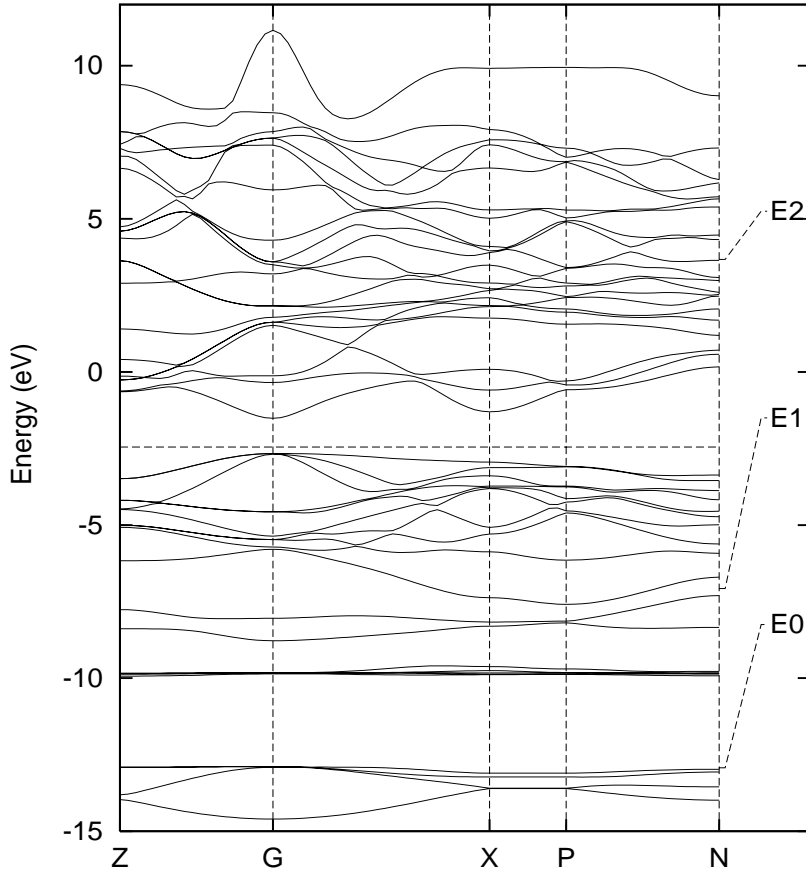


Figure 3. The band structure of $ZnIn_2Te_4$ within the NMTO

the Te-s electrons. The sharp peak at -10 eV is due to the very narrow Zn-d bands. The next structures around -8 eV arise from the In-s and Zn-s electrons. The predominantly covalently bonded Te sp states gives rise to bonding and anti-bonding bands around -5 eV and 5 eV respectively. The band gap lies between these bands.

2.2. Optical Properties:

In recent years a number of methods have been proposed for calculating optical properties within the framework of the LMTO [21, 22, 24, 26] for both metals [21, 22] and semi-conductors [23, 25, 26]. Upenski *et al* [21] proposed a method for the accurate calculation of the optical matrix elements based on the continuity equation for the charge -density operator. They were able to calculate accurate optical matrix elements by including the combined correction term to compensate for inaccuracies in the wavefunction due to the basis set in LMTO theory being finite. This method and corrections were subsequently applied by other authors [22, 23] to calculate accurate optical spectra of Ge, GaAs, InSb and CdTe.

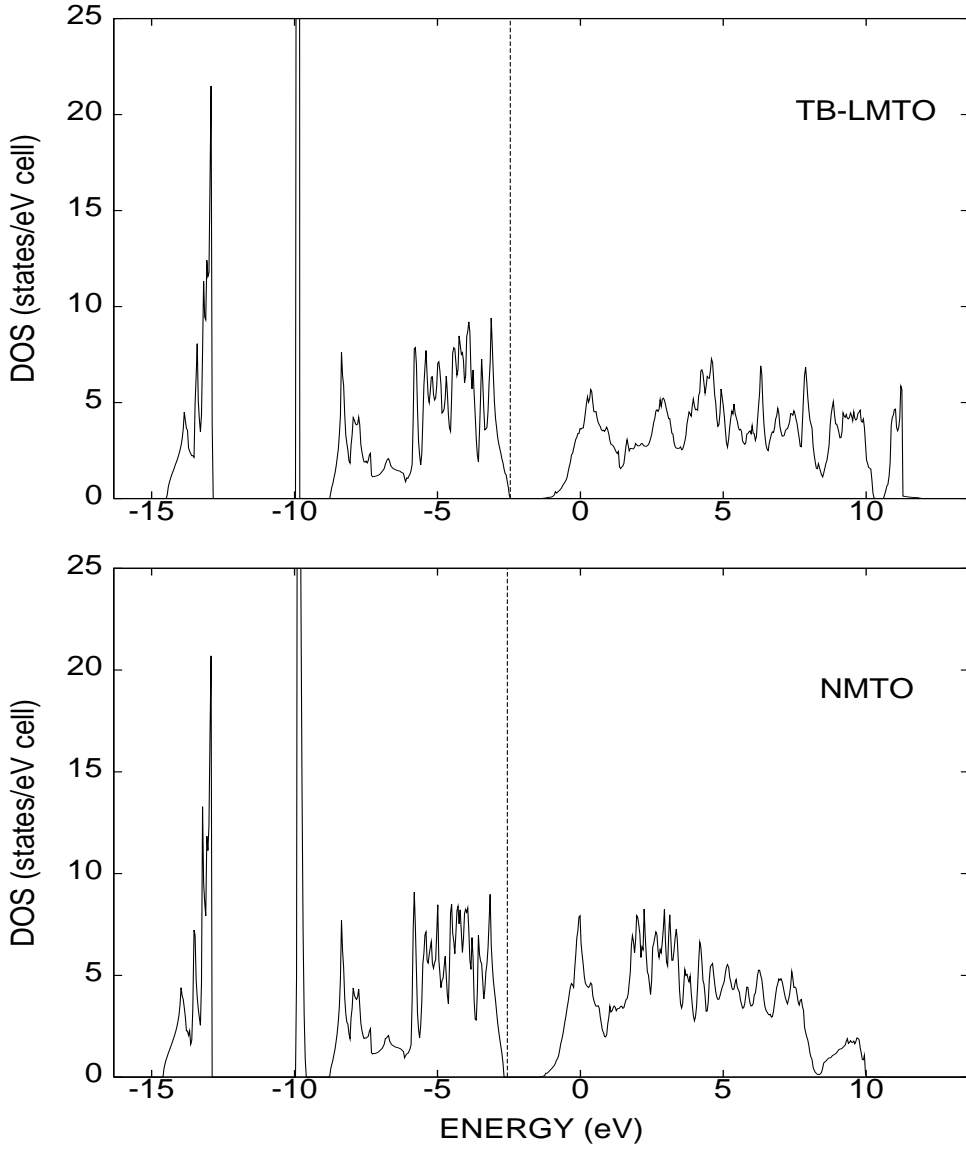


Figure 4. Density of States for $ZnIn_2Te_4$ (top) calculated from the TB-LMTO and (bottom) calculated from NMTO with three nodal energies across the energy range

In all the above calculations however, the gradient operator has been employed for the determination of the optical matrix. There is an alternative method developed by Hobbs *et al* [26] which avoids the determination of gradient operator. Their method allows for the inclusion of non-local potentials in the Hamiltonian. In their method they employed Green's second identity and the commutation relation between the position and Hamiltonian operators. They finally wrote the momentum matrices in terms of Gaunt coefficients [28] and potential parameters which are defined within the LMTO method [16, 19]. The mathematics has been described in detail both by Hobbs *et al* and by Saha *et al* ([30]). We shall indicate here the minor changes required for the calculation of the transition matrix element within the NMTO.

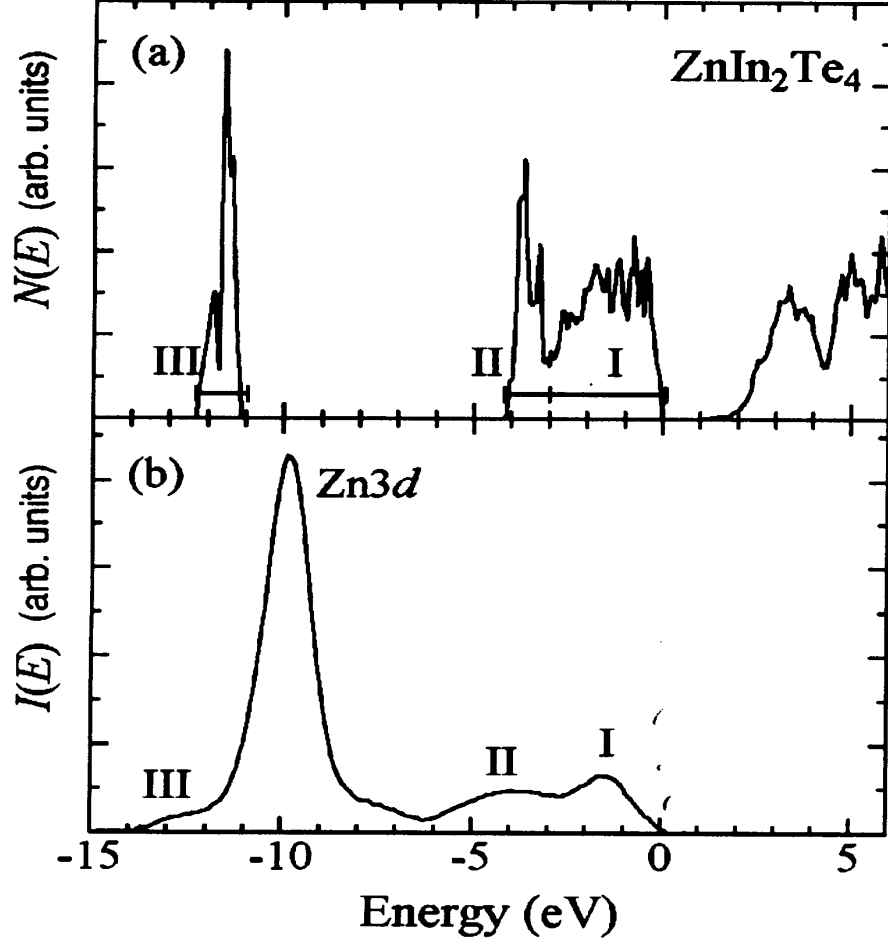


Figure 5. (a) Theoretical density of states $N(E)$ and (b) experimental XPS spectrum $I(E)$ taken from Ref. [5]

The expression for the imaginary part of the dielectric response remains the same, as derived from the Kubo formula :

$$\epsilon_2^\gamma(\omega) = \frac{-8\pi^2 e^2}{2m^{*2}\Omega} \frac{1}{\omega^2} \sum_i \sum_f |\langle \psi_f | \hat{e}_\gamma \cdot \hat{p} | \psi_i \rangle|^2 F_i (1 - F_f) \delta(E_f - E_i - \hbar\omega) \quad (3)$$

where, m^* is the effective mass of the electron, Ω is the volume of the sample, i and f refer to the initial and final states respectively, γ refers to the direction of polarization of the incoming photon, \hat{p} is the momentum of the electron and $F_{i,f}$ is the occupation probability of the initial and final states respectively. For semiconductors, i lies in the valence band and f in the conduction band and at 0^0K we have $F_i = 1$ and $F_f = 0$.

We can obtain the real part of the dielectric function $\epsilon_1(\omega)$ from a Kramers-Krönig relationship.

$$\epsilon_1(\omega) = 1 + \frac{2}{\pi} \int_0^\infty \frac{(\omega' - \omega) \epsilon_2(\omega')}{\omega'^2 - \omega^2} d\omega' \quad (4)$$

The transition probability which involves momentum matrix elements can be evaluated using a gauge independent formalism and commutation relation

$$\mathbf{P} = m_e \frac{d\mathbf{r}}{dt} = \frac{m_e}{i\hbar} [\mathbf{r}, H]$$

Thus calculation of momentum matrix elements means calculation of the following integrals:

$$\int \phi_{nL'}^\alpha(\mathbf{r})^* \mathbf{r} H \phi_{nL}^\alpha(\mathbf{r}) d^3\mathbf{r} \quad \& \quad \int \phi_{nL'}^\alpha(\mathbf{r})^* H \mathbf{r} \phi_{nL}^\alpha(\mathbf{r}) d^3\mathbf{r}$$

By noting the relations:

$$H \phi_{nL}^\alpha(\mathbf{r}) = \epsilon_n^\alpha \phi_{nL}^\alpha(\mathbf{r})$$

and using Green's second identity we may write the integrals as:

$$\begin{aligned} \int \phi_{nL'}^\alpha(\mathbf{r})^* \mathbf{r} H \phi_{nL}^\alpha(\mathbf{r}) d^3\mathbf{r} &= \imath^{\ell-\ell'} \epsilon_n^\alpha \mathbf{\Gamma}_{LL'} \int_0^{s_\alpha} \phi_{n\ell'}^\alpha(r) \phi_{n\ell}^\alpha(r) r^3 dr \\ \int \phi_{nL'}^\alpha(\mathbf{r})^* H \mathbf{r} \phi_{nL}^\alpha(\mathbf{r}) d^3\mathbf{r} &= \imath^{\ell-\ell'} \mathbf{\Gamma}_{LL'} \left\{ \epsilon_n^\alpha \int_0^{s_\alpha} \phi_{n\ell'}^\alpha(r) \phi_{n\ell}^\alpha(r) r^3 dr \dots \right. \\ &\quad \dots + (\hbar^2/2m_e) s_\alpha^2 \phi_{n\ell}^\alpha(s_\alpha) \phi_{n\ell'}^\alpha(s_\alpha) (D_{n\ell'}^\alpha - D_{n\ell}^\alpha - 1) \left. \right\} \end{aligned}$$

where, s_α is the atomic sphere radius of the α -th atom in the unit cell and $\mathbf{\Gamma}_{LL'}$ is a combination of Gaunt coefficients [26] :

$$\mathbf{\Gamma}_{LL'} = \sqrt{(2\pi/3)} \left[\left(G_{\ell',1,\ell}^{m',-1,m} - G_{\ell',1,\ell}^{m',1,m} \right) \hat{\mathbf{i}} + \imath \left(G_{\ell',1,\ell}^{m',-1,m} + G_{\ell',1,\ell}^{m',1,m} \right) \hat{\mathbf{j}} + \sqrt{2} G_{\ell',1,\ell}^{m',0,m} \hat{\mathbf{k}} \right]$$

$D_{n\ell}^\alpha$ is the logarithmic derivative of $\phi_{n\ell}^\alpha(r)$ at $r = s_\alpha$

The lattice for $ZnIn_2Te_4$ does not have cubic symmetry. If we take the c -axis to be the z -axis, it is clear that the three optical responses ϵ_x , ϵ_y and ϵ_z are not the same.

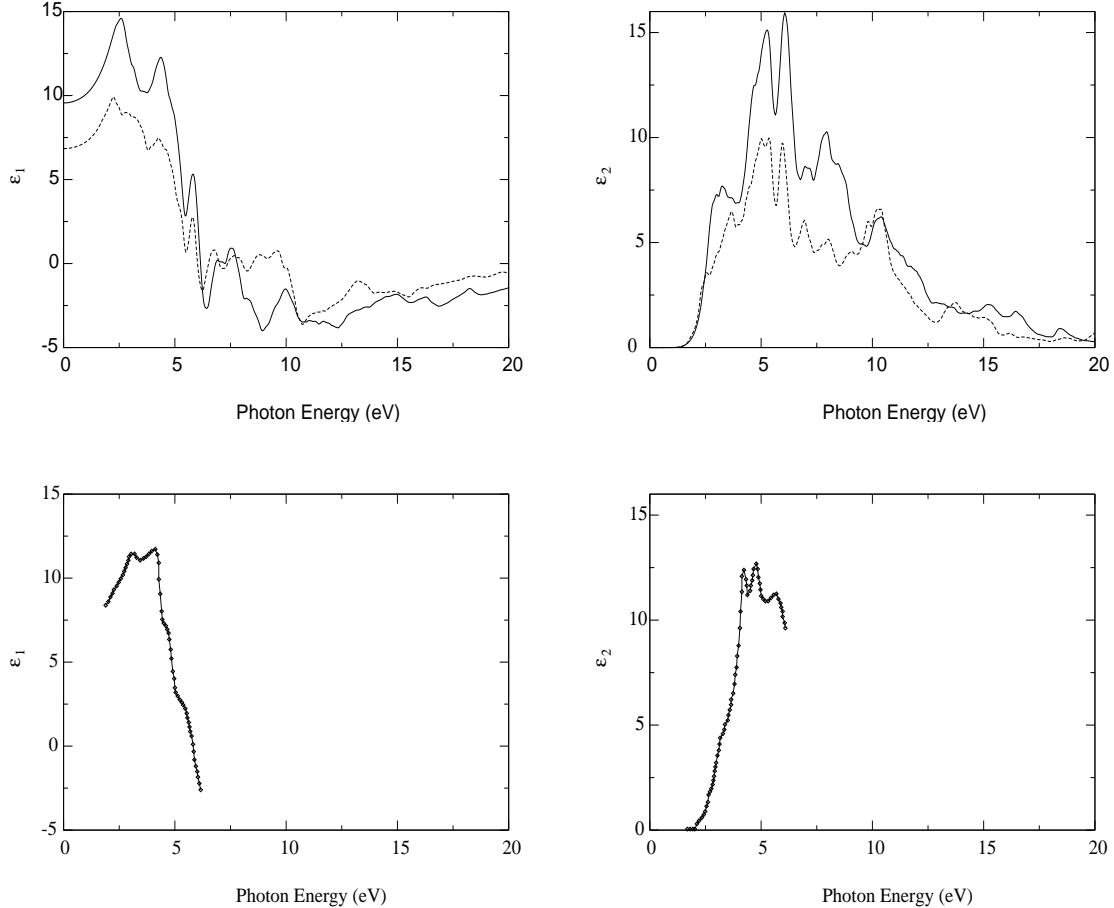


Figure 6. (Top) Real and Imaginary parts of the dielectric function of $ZnIn_2Te_4$ calculated from an NMTO calculation. The full lines show ϵ_{\perp} and the dashed lines ϵ_{\parallel} . (Bottom) The experimental results of Ozaki *et al* [5]

In the top part of figure 6, we show the variation of the real and imaginary parts of $\epsilon_{\parallel} = \epsilon_z$ and $\epsilon_{\perp} = \epsilon_x + \epsilon_y$ with the incident photon energy

We first note that since our LDA-based calculations give a smaller band gap than experiment, we have applied the *scissors* operator, which involves a rigid shift of the conduction band with respect to the valence band, so that the band gap matches. This is frequently used by LDA practitioners, but cannot be fully justified. The correct procedure would be to carry out a full GW calculation which gives rise to an *energy dependent* self-energy, which shifts the bands unequally at different energies, resulting in a distortion of the shape of the densities of states as well. Given this, the agreement of the theoretical calculations with the experimental results of Ozaki *et al* [5] available up to 10 eV photon energies, is not bad. The experiment does not align the crystal axis with the polarization of the electric field, so that we should compare the results the direction averaged response $(\epsilon_{\parallel} + \epsilon_{\perp})/3$. The principal peak positions and heights are well reproduced.

We shall conclude with the remark on the two directions which we propose to take from here. The first point is to recognize that the NMTO calculations form a reasonable starting point of the more sophisticated many-body GW approaches. The second is related to the reason why we chose to study the defect chalcopyrite in the first place. We would like to fill the voids in the structure with various “impurities” and study the signal for these in the optical response. These will be the aim of our subsequent work in this area.

Acknowledgments

We would like to thank Prof. O.K. Andersen for kind permission to use the NMTO codes developed by his group. Financial help from the University of Warwick is also gratefully acknowledged.

References

- [1] Georgobiani A.N., Radautsan S.I., and Tiginyanu I.M., 1985 *Sov. Phys. Semicond.* **19**, 121
- [2] Hahn H., Frank G., Klingler W., Störger A.D., and Störger G., 1955 *Z. Anorg. Allg. Chem.* **279** 241
- [3] Madelung O., in *Numerical Data and Functional Relationship in Science and Technology*, ed. by O. Madelung, *et al* **17** (Springer, Berlin, 1985)
- [4] Matsumoto Y, Ozaki S., and Adachi S., 1999 *J. Appl. Phys.* **86** 3705
- [5] Ozaki S., and Adachi S., 2001 *Phys. Rev.* **B64** 085208
- [6] Neumann H., Kissinger W., Lévy F., Sobotta H., and Riede V., 1990 *Cryst. Res. Technol.* **25** 841
- [7] Neumann H., Kissinger W., and Lévy F., 1990 *Cryst. Res. Technol.* **25** 1189
- [8] Boltivets N.S., Drobayazko V.P., and Mityurev V.K., 1969 *Sov. Phys. Semicond.* **2** 867
- [9] Manca P., Raga F., and Spiga A., 1973 *Phys. Status Solidi* **A16** K105
- [10] Manca P., Raga F., and Spiga A., 1974 *Nuovo Cimento Soc. Ital. Fis.* **B19** 15
- [11] Meloni F., Aymerich F., Mula G., and Baldereschi A., 1976 *Helv. Phys. Acta* **49** 687
- [12] Myers S.M. et.al, 1992 *Review of Mod. Phy.* **64** 559 (*****)
- [13] Domain C, and Becquart C.S., 2001 *Phys. Rev.* **B65** 024103
- [14] Hohenberg P., and Kohn W., 1964 *Phys. Rev.* **136** 864B
- [15] Kohn W., and Sham L.J., 1965 *Phys. Rev.* **140** A1133
- [16] Andersen O. K. 1975 *Phys. Rev.* **B12** 3060
- [17] Jepsen O. and Andersen O. K. 1971 *Solid State Commun.* **9** 1763
- [18] Andersen O. K. and Saha-Dasgupta T. 2000 *Phys. Rev.* **B62** R16219
- [19] Skriver H. L. 1984 *The LMTO Method: Muffin Tin Orbitals and Electronic Structure* (New York: Springer)
- [20] Barth U., and Hedin L., 1972 *J. Phys. C: Solid State Phys.* **5** 1629
- [21] Uspenski Yu A., Maksimov E.G., Rashkeev S.N. and Mazin I.I., 1983 *Z. Phys.* **B 53** 263
- [22] Alouani M., Koch J.M. and Khan M.A., 1986 *J. Phys. F: Met. Phys.* **16** 473
- [23] Alouani M., Brey L. and Christensen N.E., 1988 *Phys. Rev.* **B 37** 1167
- [24] Zemach R., Ashkenazi J. and Ehrenfreund E., 1989 *Phys. Rev.* **B 39** 1884
- [25] Zemach R., Ashkenazi J. and Ehrenfreund E., 1989 *Phys. Rev.* **B 39** 1891
- [26] Hobbs D., Piparo E., Girlanda R. and Monaca M., 1995 *J. Phys. C: Solid State Phys.* **7** 2541
- [27] Aulber. W.G., et.al. "Quasiparticle Calculations in Solids" p. 1-218 in "Solid State Physics" **54** edited by Ehrenreich, H. and Spaepen, S. (Academic Press) and reference therein (*****)

- [28] Rose M.E., 1957 *Elementary Theory of Angular Momentum* (New York: Wiley)
- [29] Ganguli B. and Mookerjee A., 2000 *Int. J. Mod. Phys. B* **14** 1537
- [30] Saha K.K., Saha-Dasgupta T., Mookerjee A., Saha S., and Sinha T.P., 2002 *J. Phys. C: Solid State Phys.* **14** 3849